Solar Energy Materials 10 (1984) 171–186
North-Holland, Amsterdam

PREPARATION OF LOW DEFECT GRADE a-Si:H FILMS BY RF MAGNETRON SPUTTERING TECHNIQUE

W. MÜLLER, J. PIRRUNG, B. SCHRÖDER and J. GEIGER

Fachbereich Physik, Universität Kaiserslautern, D-6750 Kaiserslautern, Fed. Rep. Germany

Received 12 January 1984

Hydrogenated amorphous silicon films have been prepared by reactive rf magnetron sputtering in an argon–hydrogen atmosphere using a ring magnetron (S-gun) as well as a planar magnetron. The main feature of the sputter unit was the conception of an all-metal bakeable vacuum system with a large target–substrate distance, to thermalize the silicon particles depositing on the substrate. The electrical properties of the films (dark conductivity, photoconductivity) turned out to depend sensitively on the hydrogen partial pressure p_{H_2}. Films prepared with the planar magnetron at $p_{H_2} = 4.6 \times 10^{-4}$ Torr and a substrate temperature $T_S = 550$ K showed best photoconductivity and highest ratio to the dark conductivity. Material deposited with this hydrogen partial pressure could be called a binary silicon–hydrogen alloy. The hydrogen content of these films amounts to about 12 at% determined by proton scattering and by hydrogen evolution technique. Infrared absorption studies showed that hydrogen is incorporated as a Si–H configuration exclusively. Sensitization, infrared and thermal quenching which was observed in the temperature dependence of the photoconductivity, was explained qualitatively with the help of a two-level model of recombination centers with different capture cross sections.

1. Introduction

Most activities and results in amorphous-silicon (a-Si) physics have been reported in the past on glow discharge (gd) deposited material [1,2]. The decomposition of silane in a glow discharge produces an amorphous material, whose electronic density of states in the midgap is of the order 10^{15}–10^{16} $cm^{-3}eV^{-1}$ if the temperature of the substrate is kept between 500–600 K. At this temperature, a considerable amount of hydrogen is incorporated into the film, passivating most of the defect states within the gap. Gd–a-Si:H proved to be the most suitable material for photovoltaic and other applications.

In contrast to that, deposition of a-Si by the sputtering technique requires additional provision for defect passivation, if a dopeable and photoelectrically applicable a-Si material is desired. A number of preparation parameters have to be optimized, in order to produce a material comparable to gd deposited films. The manipulation of numerous independent parameters, of course, makes the process of preparation more complex, but there is some hope that it should open up new possibilities of improving the properties of the material and obtaining an additional physical understanding of it.

Since the sputtering technique is well known in industrial application and

practical experiences exist for large area fast deposition of thin films, this method could become important for the fabrication of a-Si : H thin film solar cells.

The first sputtered films of amorphous Si were reported by Paul, Connell and Temkin [3] to have a large number of defects (dangling bonds etc.) which gave rise to a high density of states in the gap between the valence band and the conduction band. Paul, Lewis, Connell and Moustakas [4] have shown that hydrogen can be incorporated into the a-Si films by reactive sputtering in an argon–hydrogen atmosphere. Under appropriate conditions, the hydrogen saturates most of the dangling bonds, enables a successful doping [4] and lowers the density of recombination centers for photogenerated charge carriers [5,6]. Detailed results on the method of preparation, the passivation of the defects by hydrogen, the doping and the charge transport properties were published by Moustakas [7] and by Anderson and Paul [8,9]. Also the properties of p–i–n and Schottky junctions prepared by sputtered a-Si and its possible photovoltaic application have been studied [10]. Moustakas and Friedman [11] reported on the remarkable efficiency of sputtered solar cells.

Although the sputtering preparation may be well controlled in general, the understanding in detail is still unsatisfactory. Many authors report on problems encountered when attempting to prepare sputtered films with reproducible properties. Also the role of hydrogen is not yet sufficiently understood, since good films contain much more hydrogen than required for the compensation of the available dangling bonds. Finally, in spite of an adequate hydrogen concentration, sputtered a-Si : H films show widely varying transport properties, since the influence of the preparation parameters on the different hydrogen bonding configurations [12,13] as well as on structural inhomogeneities and film growth conditions [6] play an important role.

All the aforementioned basic papers were concerned with preparation by *diode* sputtering. The present work describes the results of a study on the influence of the deposition conditions on the properties of intrinsic rf *magnetron* sputtered material.

2. Experimental

2.1. The sputter system

Since the sensitivity of a-Si : H film properties to the deposition conditions is well known, the sample preparation was carried out in a UHV sputter system, under conditions which are known as accurately as possible.

A schematic view of the sputter system is given in fig. 1. It was based on a commercial Varian UHV evaporation system. The commercial Varian S-gun as well as a self-designed planar magnetron have been made compatible with the UHV technique. The system was pumped by ion pumps with a total pumping speed of 770 $l\ s^{-1}$ and a turbomolecular pump (270 $l\ s^{-1}$). The ion pumps could be separated from the sputtering chamber by the main valve. They were used for pumping down the system only and were never exposed to higher pressure or to reactive gases.

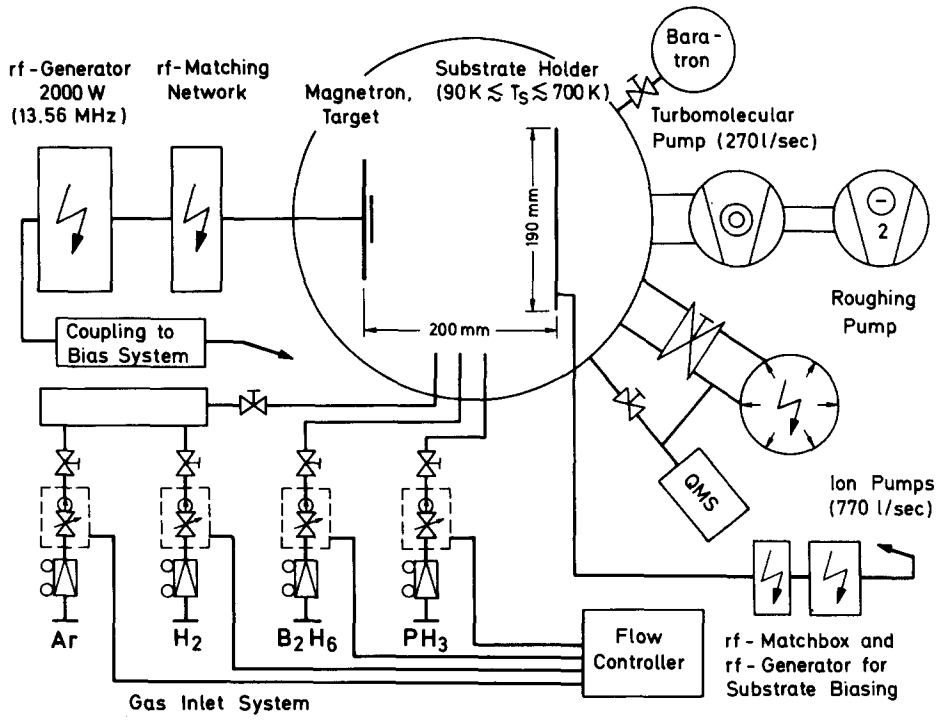

Fig. 1. Schematic view of the magnetron sputter system. QMS: quadrupole mass spectrometer.

During sputtering, only the turbomolecular pump (270 l s^{-1}) was operating. To provide a quick substrate exchange, the system was pumped down by the turbo pump to below 5×10^{-8} Torr without baking. With baking and with the supplementary ion getter pumps in action, a final pressure in the 10^{-10} Torr range could be obtained. Residual gas analysis was carried out by a UTI quadrupole mass spectrometer. During the sputtering process, a separately pumped receptacle connected to the main chamber via a throttle valve was used, where the pressure was maintained sufficiently low for the quadrupole mass spectrometer. Argon, hydrogen and doping gases were supplied to the vacuum system by short stainless steel tubes through flow controllers. Argon and hydrogen were premixed before the inlet, while the doping gases were admitted through separate lines to reduce intermixing effects when the doping gas had to be changed. Since the film properties appeared to be extremely sensitive, in particular to the hydrogen partial pressure, the absolute pressure was always measured by a capacitive vacuum gauge (baratron) with high accuracy.

Argon and hydrogen with a purity of 99.9999% have been used. As shown by a mass-spectroscopical analysis, the injection of argon did not alter the background vacuum, while hydrogen injection led to a noticeable increase of some residual gas species like H_2O and CO, possible caused by desorption processes. Flushing and baking of the feed tubes finally enabled a preparation with a background pressure of

about 10^{-7} Torr in the unbaked system and less than 10^{-8} Torr in the baked system.

The substrate holder could be heated up to about 700 K, but also cooled down to liquid nitrogen temperature. During sputtering, an electrical floating of the substrate holder was preferred, leading to a self-biased substrate potential of about +10 V above ground (wall). A rotatable shutter enabled the coating of six different substrate sections, one after the other, during a deposition run. Therefore, six films could be prepared under the same conditions during one cycle.

The thickness of the sputtered silicon films was of the order of 0.5 μm. The films were usually deposited onto sapphire substrates coated with chromium contacts 1 mm apart for the electrical measurements. Ohmic behaviour of the samples was always observed for electric field strengths of about 1 kV cm^{-1}.

Infrared absorption measurements were carried out with films on polished single-crystalline silicon wafers or KBr, by means of the Nicolet FT-spectrometer MX1.

A He–Ne laser in connection with phase-sensitive detection or with a Keithley 610C electrometer was used for photoelectric measurements. The power of the He–Ne laser was 0.6 mW cm^{-2}, corresponding to 1.9×10^{15} photons cm^{-2} at wavelength $\lambda = 632$ nm. The electrometer was fitted with automatic range selection, to carry out the measurement completely computer controlled.

2.2. Magnetron sputtering sources

As already reported in the literature [14,15], magnetron sputtering provides numerous advantages compared to conventional diode sputtering. The main benefits are higher deposition rates, higher efficiency for reactive sputtering in a hydrogen–argon atmosphere and considerably lower particle energies. Despite the increase of the deposition rate by a factor 5 to 10, the self-bias potential is lower than in the case of conventional diode sputtering. Therefore, the lower energy of the particles in the plasma diminishes possible damage by energetic particles hitting the growing film. In addition, the magnetic field traps the electrons, preventing radiation damage by these electrons, as well as uncontrolled heating of substrate and film. Furthermore, the magnetron technique allows large target–substrate distances at reasonable sputtering rates and low pressure operation. For the geometry shown in fig. 1, the target–substrate distance is set to 20 cm, leading to the uniform covering of an area of at least 200 cm^2.

The two magnetron sputtering sources have been used alternatively for preparation. Both sources were operated at a target self-bias potential of about −1000 V, which adjusted itself even at rather low target power densities (see below), since the permanent magnetic field was weak (0.015 T). According to eq. (4) of the paper by Anderson et al. [16], which followed from kinetic considerations by Westwood [17], complete thermalization is expected for a maximum particle energy of 1000 eV at a distance of 20 cm, for an argon pressure of $\gtrsim 3$ mTorr. At lower argon pressures, particles with an energy somewhat higher than thermal still arrive at the substrate. Hence the total pressure was set to 3 mTorr in most cases.

The first source, the S-gun commercial ring magnetron [18], was operated at a

sputtering power of 1500 W, corresponding to a target power density of 13 W cm^{-2}. Specially shaped polycrystalline Si targets with a purity of 99.999% were used. Sputter and reactive gases were directly introduced into the anode–cathode space. Typical deposition rates of 20 nm min^{-1} have been achieved for the conditions described above. The deposition rate increased to 60 nm min^{-1} for a target–substrate distance of 8 cm. In the second source, the planar magnetron, a single-crystalline silicon disc, 10 cm in diameter with a thickness of about 1 cm, was used as a target. The self-bias target potential of -1000 V appeared for a sputtering power of 700 W (11 W cm^{-2}), leading to deposition rates around 18 nm min^{-1}. Water cooling was achieved directly via the metallized backside of the target disc. Either magnetron was operated by a 13.6 MHz rf power supply, which enables very stable plasma conditions within the range of parameters studied so far.

3. Experimental results and discussion

3.1. The role of the argon pressure

In conventional diode sputtering systems, the argon pressure mainly influences the sputtering rate and the thermalization of the plasma particles, thereby determining the film growing conditions, the film porosity and the stability of the a-Si film. Anderson et al. [16] found that rather high argon pressures are necessary to obtain a material with a low density of states in the gap. The authors attributed this to a reduction in energetic silicon atom bombardment of the growing film with increasing argon partial pressure. There was, however, an upper limit beyond which the photoelectric properties get worse. During the course of the present work it was found that rf magnetron sputtering is scarcely sensitive to a variation of the argon pressure between 1 and 20 mTorr. Thus, for the geometry of fig. 1, this pressure could be reduced down to about 1 mTorr seemingly without an appreciable increase in bombardment-related damage for a target potential of ~ -1000 V. By keeping the argon pressure between 1 and 3 mTorr, the incorporation of argon remained at a very low level. The argon concentration, determined by means of the Rutherford backscattering technique, was between 0.5 and 1 at%, independent of the particular sputtering conditions [20]. From evolution measurements carried out by Beyer [21], an argon concentration of less than 0.1% was found, if the films had been annealed up to 800 °C. The positive self-bias potential of the floating substrate holder may have favourably contributed to the exceptionally low argon content of the magnetron-sputtered silicon films.

3.2. The role of the hydrogen pressure

The efficient passivation of the electrically active defects in the amorphous Si network has to be accomplished [4,5] by sputtering in an argon–hydrogen mixture. This way, the electric dark conductivity σ_D is reduced by many orders of magnitude and the photoconductivity σ_{ph} can be considerably increased if the sputtering process is carried out at the proper hydrogen pressure. The photoconductivity σ_{ph} is

understood here as the difference between the conductivity under illumination and the dark conductivity. A careful study of the dependence of the quantities $\sigma_{D,RT}$ and $\sigma_{ph,RT}$ on the partial pressure of hydrogen for our magnetron sputtering system has shown that this dependence is rather complex (see fig. 2 for the S-gun). At increased substrate temperatures $T_S = 575$ K, the general decrease of the dark conductivity at room temperature $\sigma_{D,RT}$ with increasing hydrogen pressure p_{H_2} is interrupted by a sharp intermediate maximum of $\sigma_{D,RT}$ within the narrow pressure range $1.5 \times 10^{-4} \leq p_{H_2} \leq 4 \times 10^{-4}$ Torr. The dark conductivity rises by two orders of magnitude and then falls to a minimum value of $\sigma_{D,RT} = 2 \times 10^{-11}$ $(\Omega\ \mathrm{cm})^{-1}$ at $p_{H_2} = 10^{-3}$ Torr. The photoconductivity at room temperature $\sigma_{ph,RT}$ shows, with increasing hydrogen pressure, a sharp intermediate maximum, which is located close to but definitely below the dark conductivity maximum. The maximum photoconductivity is more than three orders of magnitude higher than the optimum value of films prepared on a room-temperature substrate.

The maximum value of the photoconductivity, which should also be a measure of a low density of states in the mobility gap, indicates that a well-defined material with distinct properties is formed, which will be called a silicon–hydrogen alloy or, later, sp-a-Si, type B.

A similar behaviour of the conductivities $\sigma_{D,RT}$ and $\sigma_{ph,RT}$ as a function of hydrogen pressure was also obtained for films deposited with the planar magnetron.

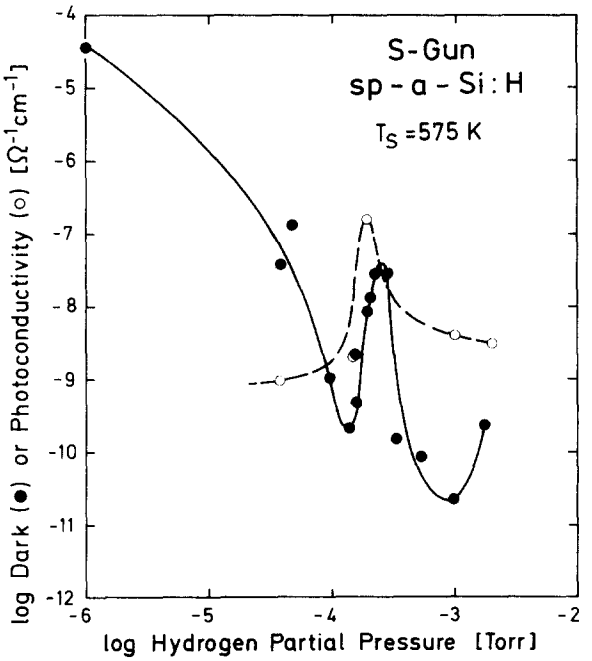

Fig. 2. The dark conductivity $\sigma_{D,RT}$ and the photoconductivity $\sigma_{ph,RT}$ at room temperature as a function of the hydrogen partial pressure for a-Si:H sputtered with the S-gun. The total pressure was $p = 3$ mTorr, the substrate temperature $T_S = 575$ K.

A corresponding diagram is given in fig. 3 with an extended scale in the region of interest of the hydrogen partial pressure. The peaks of σ_D and σ_{ph} are again located in the same order, but at a somewhat higher hydrogen pressure compared to the S-gun, which may be due to the changed geometry of the source and the different operational conditions. From the analyses of the films, however, the hydrogen content turned out to be the same (see section 3.3). So far, the best values of photoconductivity were obtained using the planar magnetron. The photoconductivity was almost one order of magnitude higher than that of films prepared by the S-gun. Related to AM1 illumination, $\sigma_{ph,RT} \approx 1 \times 10^{-4}$ $(\Omega\ \mathrm{cm})^{-1}$ has been obtained at the maximum, which is of the same order as the best results which have been observed for undoped samples prepared by diode sputtering [6] or by the glow-discharge method [2,22,23]. Following Street [23], ESR spin density values less than 10^{16} cm^{-3} can be derived from this optimum photoconductivity. Also the high ratio $\sigma_{ph,RT}(AM1)/\sigma_{D,RT} = 3 \times 10^4$ indicates a material which is low in defects and favourable to photovoltaic applications.

With reference to figs. 2 and 3, a possible interpretation of the dependence of the

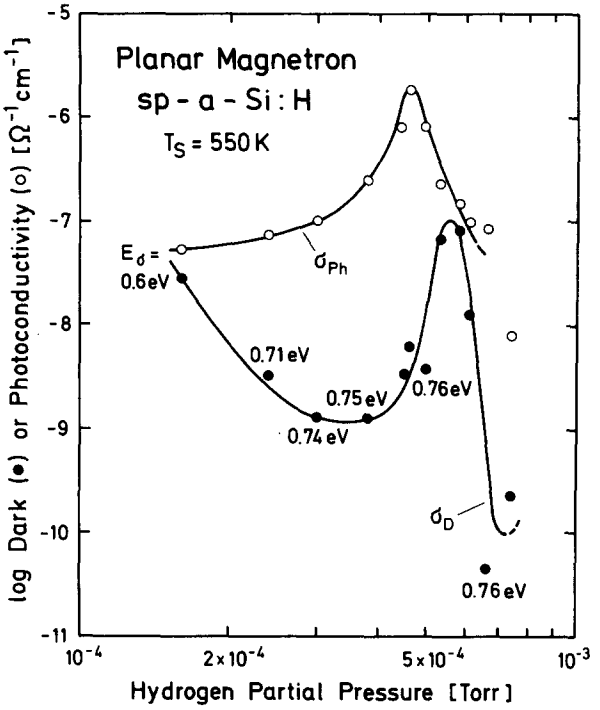

Fig. 3. The dark conductivity $\sigma_{D,RT}$ and the photoconductivity $\sigma_{ph,RT}$ at room temperature as a function of the hydrogen partial pressure for a-Si:H sputtered with the planar magnetron. The total pressure was $p = 3$ mTorr, the substrate temperature $T_S = 550$ K. The numbers give the activation energy E_σ of the dark conductivity, determined from its temperature dependence, if the conductivity is activated around room temperature.

electrical properties on the hydrogen partial pressure for the reactive magnetron sputtering will be given in the following paragraphs.

With increasing hydrogen partial pressure, more and more hydrogen will be incorporated into the silicon network of the film. In this way, to an increasing degree, the remaining free bonds and other structural or stoichiometric defects tend to be saturated or deactivated by hydrogen. The dark conductivity, which was first dominated by hopping transport in localized states near the Fermi level characterized by a temperature dependence $\sigma_D \sim \exp(T^{-1/4})$ over a wide temperature range, becomes thermally activated at lower and lower temperatures. Finally, σ_D is thermally activated over the whole measuring range for $p_{H_2} \approx 10^{-4}$ Torr. At higher pressures the room-temperature dark conductivity decreases steadily, since the thermal activation energy $E_\sigma = E_c - E_F$ (E_c: energy at the mobility edge of the conduction band, E_F: Fermi energy) increases. This increase of E_σ may be due to either a downward shift of the Fermi level E_F, or an upward shift of the mobility edge E_c. The latter would correspond to the analogous shift of the conductivity mobility edge E_c with increasing incorporation of hydrogen in gd-Si samples [24]. The photoconductivity σ_{ph} is still very small. Apparently, the defect states are passivated such that positively charged defect states still remain in the upper half of the gap, which interact with the photoelectrons as recombination centers with a large cross section.

Disregarding the peaks of the dark conductivity and photoconductivity in figs. 2 and 3, the trend described above would continue up to a hydrogen partial pressure of about 10^{-3} Torr. So one could speak of a particular sp-a-Si phase or modification, which we call "type A". This material is probably rather inhomogeneous.

On to this background, the peak is superimposed. In this narrow hydrogen partial pressure range with a width of about $2-3 \times 10^{-4}$ Torr corresponding to a hydrogen content of 10–15 at% (see section 3.3), we propose a second modification to be formed with new properties, which we call "type B". With increasing hydrogen pressure, the photoconductivity increases strongly. A possible explanation would follow the model of Anderson and Spear [22] which was also used by us for the explanation of the annealing behaviour of a-Si:H films evaporated in an atmosphere of hydrogen [25]. The idea is that we are dealing with an unintentional doping and thereby neutralizing positively charged defect states with a high recombination cross section. This model, however, cannot easily explain the subsequent decrease of the photoconductivity, which is accompanied by a peak in the dark conductivity.

It seems to us much more likely that a recombination model as developed by Rose [26] and later applied to the characterization of the photoconductivity of undoped gd-a-Si:H by Wronski and Daniel [27] has to be applied for at least a qualitative understanding of the behaviour of our films of type B. For a quantitative explanation, further and more detailed studies are required. In its simplest form, this model consists of two levels of recombination centers located energetically below and above the dark Fermi level (fig. 4). In amorphous silicon, these levels should be more or less broad distributions. It is supposed that the photocurrent is carried by electrons. The upper recombination centers (class I) have large capture cross sections

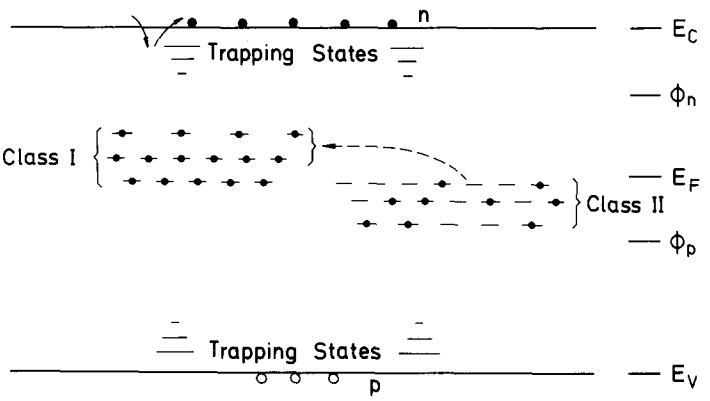

Fig. 4. Schematic energy diagram of the two-state model for explaining the sensitization (and the quenching) of the photoconductivity in sp-a-Si:H. The class I states, by themselves, lead to fast recombination, the class II states, by themselves, lead to slow recombination. The dashed arrow indicates the arrangement of the electrons under illumination, passivating the class I recombination centers. E_c and E_v are the mobility edges of the conduction and valence band, E_F the dark Fermi level and ϕ_n and ϕ_p the quasi-Fermi levels of the electrons and the holes. The states are drawn separately to avoid confusion. In reality they are interspersed.

for electrons and the lower centers (class II) very small ones. The strength of illumination is supposed to be such that the two classes of recombination centers are between the quasi-Fermi levels.

Beginning at low hydrogen pressure for type B (say, around 0.3 mTorr in fig. 3), a material with a rather low density of gap states is deposited. The photoconductivity is limited by a certain density of recombination centers of class I with large capture cross sections. With increasing hydrogen pressure, the density of the centers of class I may be reduced, but, more importantly, we believe recombination centers of class II with an extremely small cross section are created. Under illumination, these class II states become occupied by holes. The charge neutrality condition requires that electrons are transferred to the class I states. The rate of recombination of the photoelectrons is now greatly diminished, because many recombination centers of class I with large cross sections are already occupied by electrons and hence, their effective density is reduced. The capture cross section of the states of class II is small anyway. So the photoconductivity of the a-Si films is increased by adding defects acting as recombination centers with small cross sections (imperfection sensitization).

If the density of states of either class which can capture free carriers becomes large (say $> 10^{17}$ cm^{-3}), the states will interact with each other and electrons (or holes) can make transitions directly between these states by hopping processes. Hence the dark conductivity increases and its temperature dependence is no longer simply activated. This is illustrated in fig. 5, which shows the temperature dependence of the dark conductivity for an a-Si film sputtered at a hydrogen partial pressure $p_{H_2} = 5.3 \times 10^{-4}$ Torr near the maximum of the room temperature dark conductivity peak of fig. 3. For comparison, the temperature dependence of the conductivity on either side of the peak is also presented. In these cases, the

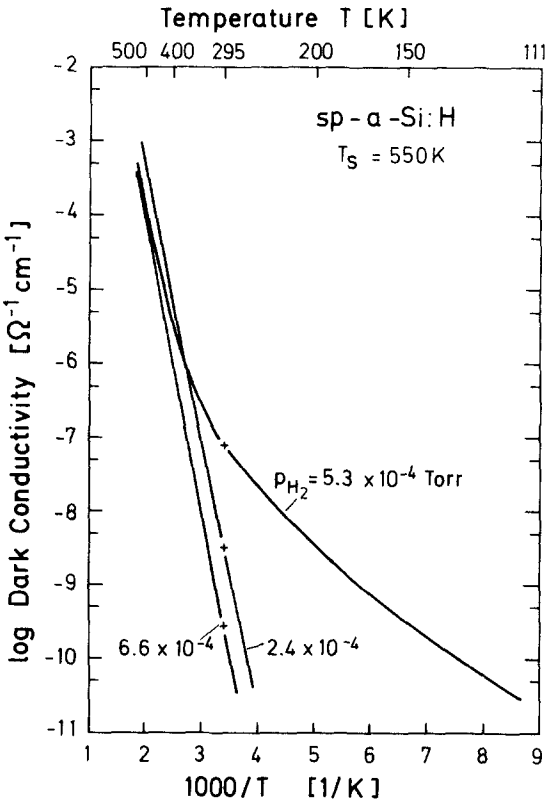

Fig. 5. The temperature dependence of the dark conductivity σ_D for a-Si:H prepared with the planar magnetron at three different values of the hydrogen pressure around the peak of the dark conductivity in fig. 3, at the top of the peak $p_{H_2} = 5.7 \times 10^{-4}$ Torr. The crosses mark the room-temperature values.

conductivity is clearly activated. For the photogenerated charge carriers, new recombination possibilities open and the photoconductivity decreases accordingly.

It should be mentioned at this point that, for films prepared at hydrogen pressures in the range of decreasing photoconductivity, thermal quenching and infrared quenching of the photoconductivity is observed. This phenomenon will be discussed in section 3.4. It is similar to the quenching effect reported by Vanier, Delahoy and Griffith [28,29] (see also ref. [30]) for gd-a-Si:H films, which appears particularly striking for films deposited at relatively low temperature (T_S = 400–500 K), where the hydrogen content is usually large. The main difference, however, is a splitting of the spectral dependence of the quenching ratio $Q = \sigma_{(V+I)}/\sigma_V$ into two peaks at low temperature [41]. $\sigma_{(V+I)}$ and σ_V are the photoconductivities with and without bias infrared illumination. Finally, if hydrogen is offered in excess, the chemistry changes and again the type A material is deposited.

The second increase of the dark conductivity in fig. 2 (and, according to preliminary results for films prepared with the planar magnetron, an increase also of the photoconductivity) at higher hydrogen partial pressure around 10^{-3} Torr is

likely due to the change of the place of reaction from the surface of the growing film to the surface of the target under the condition of high hydrogen pressure, as suggested by Moustakas [6].

3.3. Hydrogen bonding configurations and concentration

Information about the mode of incorporation of hydrogen into the magnetron sputtered films and its concentration was obtained by ir absorption spectroscopy, hydrogen evolution measurements (Beyer [21]) and by means of the elastic recoil technique. In the last-named method, a beam of 2 MeV $^4He^+$ ions was directed onto the films, knocking out hydrogen atoms which could be detected in the forward direction [31]. Details of this technique and the results of the measurements on sputtered film will be published elsewhere [20].

Fig. 6 shows the hydrogen content of the films as a function of the hydrogen partial pressure during deposition. The open circles and open squares present data measured by the elastic recoil technique. Up to $p_{H_2} \approx 5 \times 10^{-4}$ Torr, the concentra-

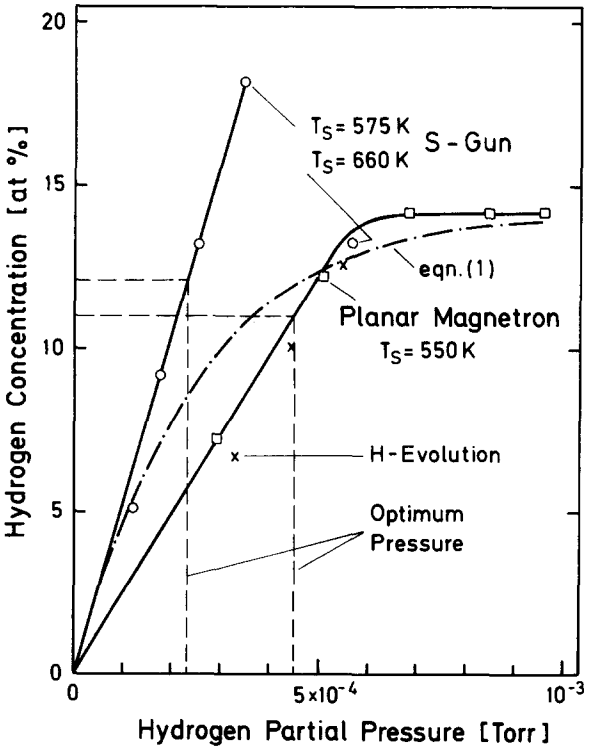

Fig. 6. The relation between the hydrogen partial pressure p_{H_2} during sputtering and the hydrogen concentration in the a-Si::H film. The open squares and circles represent the results of the elastic recoil technique [20] for films prepared with the two magnetrons. The crosses represent the results of the evolution measurements [21]. The dash-dotted line gives the functional dependence of eq. (1) for the planar magnetron.

tion of incorporated hydrogen is proportional to the hydrogen partial pressure offered. The rate of incorporation depends on the particular sputtering conditions and on the geometry and therefore is different for deposition with the planar magnetron and the S-gun. Note that optimally passivated films contain nearly the same amount of hydrogen (11–12 at%), independent of the type of magnetron used. For a hydrogen pressure above 6×10^{-4} Torr, a saturation of the hydrogen content is found for samples prepared by the planar magnetron. On the basis of a kinetic model, Moustakas [32] derived an expression for the dependence of the hydrogen concentration c_H on the partial pressure p_{H_2}:

$$c_H = (c_H)_{max}\left[1 - \exp(k \cdot p_{H_2})\right]. \tag{1}$$

The physical meaning of the constant k is explained in ref. [32]. The normalized functional dependence of eq. (1) is also plotted in fig. 6 for the films sputtered by the planar magnetron. The agreement with the measurement is only moderate. From this it can be concluded that under our conditions of magnetron sputtering, the kinetic model [32] is insufficient to describe the processes taking place at the surface of the growing film. The hydrogen concentration of the films produced by the S-gun is generally higher and the plateau is not yet attained. An increase of the substrate temperature results in a lowering of the hydrogen content, as expected.

Hydrogen evolution experiments were carried out for our sputtered films by Beyer [21], with the following results: for samples deposited with the planar magnetron, the hydrogen content agrees with those values determined by the elastic recoil technique (see crosses in fig. 6). The evolution of hydrogen occurs only between 400 and 700 °C with no indication of a low-temperature evolution maximum. This means the hydrogen incorporated in the film is chemically bound without exception. The temperature at the maximum evolution rate T_M varies with the thickness of the film. This behaviour is characteristic for a limitation of the evolution by diffusion, as it is known from samples prepared by glow discharge in silane [33]. Also the absolute values of $T_M = f(d)$ agree with the corresponding values for gd films.

From ir vibrational spectroscopy, information is obtained on the Si–H bonding configurations; in particular, from the spectral range of the stretching mode around 2000 cm^{-1} [13]. Fig. 7 presents the infrared absorption spectrum of an a-Si film on a KBr substrate, which was prepared under optimum conditions. The spectrum shows a strong band at 615 cm^{-1} due to the bending mode and a weaker band at 1990 cm^{-1} due to the stretching mode of Si–H. There are two additional bands at 860 and 1060 cm^{-1}, which are attributed to SiN and SiO vibrations and possibly due to reactions after deposition [6]. For either type of magnetron, no indication of a SiH_2 stretching mode at 2100 cm^{-1} could be found within a range of hydrogen partial pressure between one half or double the optimum pressure for type B. Only at unusually high hydrogen pressures, a rather weak shoulder at 2100 cm^{-1} appeared. Regardless of the interpretation of the 2100 cm^{-1} mode [34], the absorption spectra of the films show that our films of type B are compositionally homogeneous. This is in contrast to diode-sputtered films, which normally exhibit a doublet [12,13].

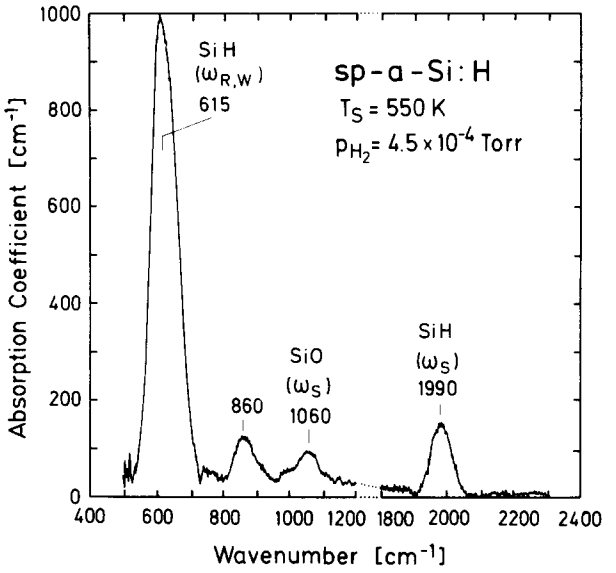

Fig. 7. Infrared absorption spectrum of a film prepared with the planar magnetron at the optimum value of the hydrogen partial pressure on a KBr substrate.

Special measure have to be taken, such as the application of a positive substrate bias [6] (for others see refs. [35,36]), to favour the Si–H stretching mode around 2000 cm^{-1}.

3.4. Temperature dependence of the photoconductivity

The temperature-dependent photoconductivity $\sigma_{ph} = f(T)$ for four samples prepared with the planar magnetron at hydrogen pressures close to the optimum value is plotted in fig. 8. The lower curve with $p_{H_2} = 2.4 \times 10^{-4}$ Torr shows the normal temperature dependence of the photoconductivity, as expected according to Spear, Loveland and Al-Sharbaty [37] for gd-a-Si:H. Since the hydrogen pressure is insufficient for an optimum sensitization of the photoconductivity, σ_{ph} remains rather low. At $p_{H_2} = 4.6 \times 10^{-4}$ Torr, the optimum hydrogen pressure is set and maximum values of the photoconductivity are measured at room temperature. With increasing hydrogen pressure, the photoconductivity at room temperature decreases again as shown by the crosses in fig. 8 and by the corresponding dependence in fig. 3. From the temperature dependence of photoconductivity, however, it is evident that the decrease of the photoconductivity sets in only at a certain temperature range, depending on the hydrogen concentration. This means the recombination centers for the photogenerated charge carriers are activated by thermal excitation. This thermal quenching can again be explained by the two-level model [26] employed before (fig. 4). With increasing hydrogen pressure, more and more recombination centers of class II are created, which, because they are distributed over a

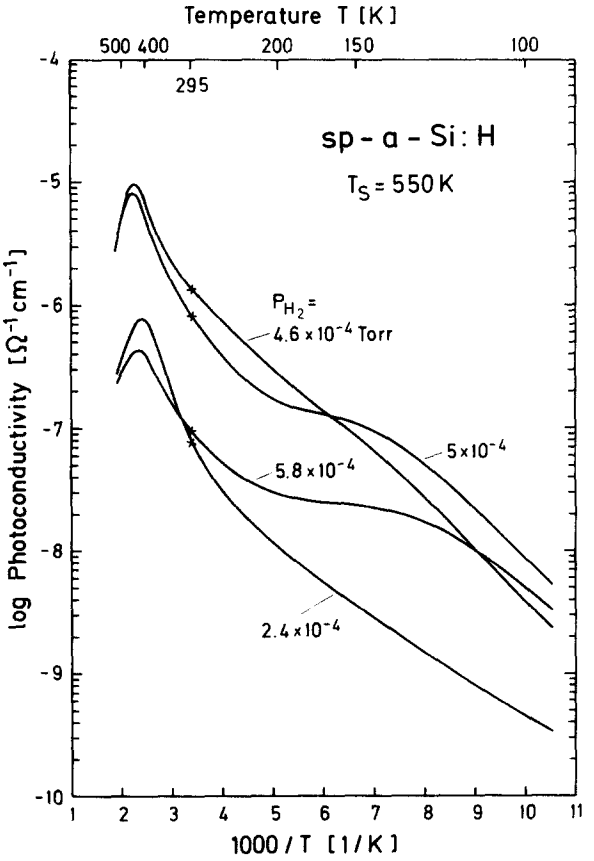

Fig. 8. Temperature dependence of the photoconductivity σ_{ph} for samples prepared at various hydrogen partial pressures p_{H_2} around the optimum p_{H_2}. The crosses mark the room-temperature values.

certain energy interval within the gap, will finally come into thermal contact with the quasi-Fermi level of the holes. Thus at low temperature and at a given level of illumination, the states of classes I and II are still located between the two quasi-Fermi levels and the photoconductor is sensitized. With increasing temperature, the quasi-Fermi levels move one against the other and in particular, the quasi-Fermi level of the holes shifts through the class II recombination centers. These states will become populated by electrons and the class I states will be emptied. These states are then able efficiently to capture photogenerated electrons and the photoconductivity decreases.

The decrease in the photoconductivity observed around room temperature and below by thermal quenching, can be accomplished also at low temperatures by bias illumination with photons $h\nu < 1.4$ eV (infrared quenching). These photons are unable to excite interband transitions. They can, however, cause electrons to make transitions from the filled valence band into the class II states and the corresponding

holes are captured by the class I recombination centers with large cross section. In this way, a rearrangement of the occupations of the two states follows just as in the case of thermal quenching.

Similar and even more pronounced thermal and infrared quenching of the photoconductivity were observed by Vanier et al. [28,29] for gd-a-Si:H. Their interpretation was based on a three-state model [38].

It should be mentioned also that irrespective of the quenching due to the creation of additional recombination centers with increasing hydrogen pressure, the shoulder at about 1.2 eV in the spectral dependence of the photoconductivity decreases. This shoulder was associated by Anderson et al. [39] with a peak in the density of states in the gap, 1.2 eV below the conduction band in the tail states of the valence band. From this it can be concluded that, with increasing hydrogen pressure, defect states at the valence band tail become saturated.

4. Conclusions

In this paper, experimental results on a-Si:H films have been presented, which illustrate that rf magnetron preparation either with an S-gun or with a planar magnetron leads to an interesting material similar to gd-deposited material. Optimum passivated films are characterized by high photoconductivity, by a large ratio σ_{ph}/σ_D and by a low density of defect states within the gap, having therefore a promising potential for photovoltaic applications [40]. It could be shown that a small variation of the hydrogen partial pressure may drastically influence the photoelectrical properties of the material. Incorporation of hydrogen exceeding the optimum amount of about 12% leads to a degradation of the photoelectrical properties, since increasing numbers of recombination centers are created. Whatever the nature of the recombination centers of either class, it follows from the present work that class II is most likely an intrinsic state of the amorphous silicon alloy and caused by the addition of hydrogen.

Acknowledgements

The authors are very grateful to Professor Dr. W. Fuhs and Dr. H. Mell of AG Halbleiterphysik, University of Marburg and their coworkers, for the preparation of several gd-films for comparison. We wish to thank Dr. W. Beyer for carrying out hydrogen evolution measurements and for helpful discussions. We also thank Stefan Iselborn and Herbert Rübel for interesting discussions. This work was supported by a grant of the Bundesministerium für Forschung und Technologie (BMFT).

References

[1] P.G. LeComber and W.E. Spear, Amorphous Semiconductors, ed. M.H. Brodsky (Springer, Heidelberg, 1979) p. 251.

[2] D.E. Carlson and C.R. Wronski, Amorphous Semiconductors, ed. M.H. Brodsky (Springer, Heidelberg, 1979) p. 287.
[3] W. Paul, G.A.N. Connell and R.J. Temkin, Advan. Phys. 22 (1973) 529.
[4] W. Paul, A.J. Lewis, G.A.N. Connell and T.D. Moustakas, Solid State Commun. 20 (1976) 969.
[5] T.D. Moustakas, D.A. Anderson and W. Paul, Solid State Commun. 23 (1977) 155.
[6] T.D. Moustakas, Solar Energy Mater. 8 (1982) 187.
[7] T.D. Moustakas, J. Electron. Mater. 8 (1979) 391.
[8] D.A. Anderson and W. Paul, Phil. Mag. B 44 (1981) 187.
[9] D.A. Anderson and W. Paul, Phil. Mag. B 45 (1982) 1.
[10] D.A. Anderson, G. Moddel and W. Paul, J. Electron. Mater. 9 (1980) 141.
T.D. Moustakas, C.R. Wronski and D.L. Morel, J. Non-Crystalline Solids 35/36 (1980) 719.
W. Paul and D.A. Anderson, Solar Energy Mater. 5 (1981) 229; erratum: 6 (1982) 251.
[11] T.D. Moustakas and R. Friedman, Appl. Phys. Lett. 40 (1982) 515.
[12] E.C. Freeman and W. Paul, Phys. Rev. B18 (1978) 4288.
[13] M.H. Brodsky, M. Cardona and J.J. Cuomo, Phys. Rev. B16 (1977) 3556.
[14] Thin Film Processes, eds. J.L. Vossen and W. Kern (Academic Press, New York, 1978) part 2.
[15] A.R. Mirza, A.J. Rhodes, J. Allison and M.J. Thompson, J. de Phys. Suppl. 42 (1981) C4-659.
[16] D.A. Anderson, G. Moddel, M.A. Paesler and W. Paul, J. Vac. Sci. Technol. 16 (1979) 906.
[17] W.D. Westwood, J. Vac. Sci. Technol. 15 (1978) 1.
[18] Ref. [14], chap. II-3.
[19] Ref. [14], chap. II-4.
[20] H. Frey, O. Meyer, W. Müller, J.M. Pirrung and A. Turos, Appl. Phys. A, submitted.
[21] W. Beyer, KFA Jülich, private communication.
W. Beyer and H. Wagner, J. Non-Crystalline Solids 59/60 (1983) 161.
[22] D.A. Anderson and W.E. Spear, Phil. Mag. 36 (1977) 695.
[23] R.A. Street, Phil. Mag. B 46 (1982) 273.
[24] G.D. Cody, C.R. Wronski, B. Abeles, R.B. Stephens and B. Brooks, Solar Cells 2 (1980) 227.
[25] S. Iselborn, H. Rübel, J. Geiger and B. Schröder, Phil. Mag. B48 (1983) 561.
[26] A. Rose, Phys. Rev. 97 (1955) 322; Concepts in Photoconductivity and Allied Problems (Interscience, New York, 1963).
[27] C.R. Wronski and R.E. Daniel, Phys. Rev. B 23 (1981) 794.
[28] P.E. Vanier, A.E. Delahoy and R.W. Griffith, J. Appl. Phys. 52 (1981) 5235.
[29] P.E. Vanier and R.W. Griffith, J. Appl. Phys. 53 (1982) 3098.
[30] R.W. Griffith, F.J. Dampas, P.E. Vanier and M.D. Hirsch, J. Non-Crystalline Solids 35/36 (1980) 391.
[31] B. Terreault, J.G. Martel, R.G. St.-Jacques and J. L'Ecuyer, J. Vac. Sci. Technol. 14 (1977) 492.
[32] T.D. Moustakas, T. Tidje and W.A. Lanford, Tedrahedrally Bonded Amorphous Semiconductors (Carefree 1981) eds. R.A. Street, D.K. Biegelsen and J.C. Knights, AIP Conf. Proc. No. 73 (1981) p. 20.
[33] W. Beyer and H. Wagner, J. de Phys. Suppl. 42 (1981) C4-783.
[34] W. Paul, Solid State Commun. 34 (1980) 283.
[35] S. Oguz, D.K. Paul, J. Blake, R.W. Collins, A. Lachter, B.G. Yacobi and W. Paul, J. de Phys. Suppl. 42 (1981) C4-679.
[36] F.R. Jeffrey, H.R. Shanks and G.C. Danielson, J. Appl. Phys. 50 (1979) 7034.
[37] W.E. Spear, R.J. Loveland and A. Al-Sharbaty, J. Non-Crystalline Solids 15 (1974) 410.
[38] R.H. Bube, J. Phys. Chem. Solids 1 (1957) 234.
[39] D.A. Anderson, G. Moddel and W. Paul, J. Non-Crystalline Solids 35/36 (1980) 345.
[40] W. Müller, S. Iselborn, J. Pirrung, B. Schröder and J. Geiger, Proc. 5th EC Photovoltaic Solar Energy Conference, Kavouri (Athens), Greece (1983) p. 798.
[41] W. Fuhs, H.M. Welsch and D.C. Booth, Phys. Stat. Sol. (b) 120 (1983) 197.